

# Numerical Study of the Cahn-Hilliard Equation in One, Two and Three Dimensions

E. V. L. de Mello

*Instituto de Física,*

*Universidade Federal Fluminense,*

*Niterói, RJ 24210-340, Brazil*

Otton Teixeira da Silveira Filho

*Instituto de Computação,*

*Universidade Federal Fluminense,*

*Niterói, RJ 24210-340, Brazil*

(Dated: November 26, 2024)

## Abstract

The Cahn-Hilliard equation is related with a number of interesting physical phenomena like the spinodal decomposition, phase separation and phase ordering dynamics. On the other hand this equation is very stiff and the difficulty to solve it numerically increases with the dimensionality and therefore, there are several published numerical studies in one dimension (1D), dealing with different approaches, and much fewer in two dimensions (2D). In three dimensions (3D) there are very few publications, usually concentrate in some specific result without the details of the used numerical scheme. We present here a stable and fast conservative finite difference scheme to solve the Cahn-Hilliard with two improvements: a splitting potential into a implicit and explicit in time part and a the use of free boundary conditions. We show that gradient stability is achieved in one, two and three dimensions with large time marching steps than normal methods.

PACS numbers: 64.75.+g, 02.30.Jr, 02.70.Bf, 74.80.-g

## I. INTRODUCTION

The theory of the phase-ordering dynamics following a rapid cooling down (or quenching) through the critical temperature from a homogeneous or disordered phase into an inhomogeneous or ordered state has been studied for decades[1, 2, 3, 4]. This phenomenon is known as spinodal decomposition. Part of the fascination of the field is because the ordering does not occur instantaneously. Instead, a network of domains of the equilibrium phases develops, and the typical length scale associated with these domains increases with the time. In other words, the length scale of the ordered regions growth with time as the different (broken-symmetry) phases compete in order to achieve the equilibrium state. One of the leading models devised for the theoretical study of this phenomenon is based on the Cahn-Hilliard formulation[5]. The Cahn-Hilliard (CH) theory was originally proposed to model the quenching of binary alloys through the critical temperature[5] but it has subsequently been adopted to model many other physical systems which go through a similar phase separation[2, 3, 4].

Recently it has been discovered that high critical temperature superconductors have an intrinsic inhomogeneous phase which exhibit patternings which involve nanoscale regions of phase separations, often referred as stripes as revealed by neutron diffraction studies[6] and EXAFS[7]. Similar findings were measured by very fine scanning tunneling microscopy/spectroscopy (STM/S) data[8, 9] which have shown the local charge and the superconducting gap spatial variation through the differential conductance. The ubiquity of such intrinsic inhomogeneities, as well as the importance of the materials that exhibit them has motivated intense experimental and theoretical research into the details of the phenomena[10, 11, 12, 13, 14]. Recently a theory of the critical field  $H_{c2}$  based on a distribution of superconducting regions with different critical temperatures due to these intrinsic inhomogeneities has explained some nonconventional features of current data on some cuprates[15]. The manganites which exhibit a colossal magnetoresistance have also some properties which may be linked with clusters formation upon cooling or an intrinsic phase separation[16, 17]. Researches on these materials are currently being investigated by a sizable fraction of the condensed matter community. Therefore, studies based on the CH equation may be useful to understand the puzzle of the origins of such intrinsic phase separation in these materials and how it affects their physical properties. Here we want to study specifically

the Cahn-Hilliard equation and we will deal with the problem of phase separation in high- $T_c$  superconductors in another publication.

In an alloy system composed by a binary mixture we can define the local phase variable  $u(\vec{x})$  as the difference in concentration between the two (incompressible) components or simply, the concentration of one of the components over the domain  $\Omega$  ( $\vec{x} \in \Omega$ ) which represents the system. It is clear that this type of phase variable or order parameter is always conserved for an isolated system and we will use below this property as the main guide for our numerical method. In the CH theory, the time variation of the order parameter  $u(\vec{x}, t)$  is given in terms of the functional derivative of a time-dependent free-energy functional  $F(u)$  leading to an equation of motion to diffusive transport of the order parameter, namely

$$\frac{\partial u}{\partial t} = M \nabla^2 \frac{\delta f}{\delta u} \quad (1)$$

where  $f$  is the free-energy density and the (constant) mobility  $M$  will hereafter be absorbed into the time scale although there are cases in which the mobility can be a function of the position[18]. The free-energy functional is assumed, to most of the physical applications, to follow the Ginzburg-Landau (GL) form:

$$f = \frac{1}{2} \varepsilon^2 |\nabla u|^2 + V(u) \quad (2)$$

where the potential  $V(u)$  may have a double-well structure like, for instance,  $V(u) = (u^2 - 1)^2/4$  as many authors have used[19, 20, 21, 22] and, for the sake of comparison with these previous works, we will adopt it below. There are other possibilities like  $V(u) = au^2/2 + bu^4/4 + \dots$  which is more convenient for physical applications since, usually the GL free energy is a power expansion in  $u$  with coefficients ( $a, b, \dots$ ) which depend on the temperature, the applied field, and on other physical properties. It is easy to see that the above double well potential will favor two phases with densities  $u = \pm 1$ . If one uses a potential with three minima, it will appear three major phases and so on. Bray[4] pointed out that one can explore the fact that the order parameter is conserved and the CH equation can be written in the form of a continuity equation,  $\partial_t u = -\nabla \cdot \mathbf{J}$ , with the current  $\mathbf{J} = \nabla(\delta f/\delta u)$ . Therefore we may write the CH equation as following,

$$\frac{\partial u}{\partial t} = -\nabla^2(\varepsilon^2 \nabla^2 u + u - u^3) \quad (3)$$

Normally,  $0 < \varepsilon \ll 1$  because the fourth derivative term requires a large stencil and it is related with the size of the interface between regions of two different phase. To accurately

resolve these interfaces a fine space discretization  $\Delta x$  is necessary. The linear term is responsible for the interesting dynamics including the instability of constant solutions near  $u = 0$  and the nonlinear term is the one which mainly stabilizes the flow[19]. As it has already been pointed out[19, 20, 21, 22], both the  $\nabla^4$  and the nonlinear term make the CH equation very stiff and it is difficult to solve it numerically. The nonlinear term in principle, forbids the use of common Fast Fourier Transform (FFT) methods and brings the additional problem that the usual stability analysis like von Neumann criteria cannot be used. These difficulties make most of the finite difference schemes to use time steps of many order of magnitude smaller than  $\Delta x$  and consequently, it is numerical expensive to reach the time scales where the interesting dynamics occur. This is the reason why numerical simulations based on Runge-Kutta schemes had to be performed in large supercomputers[23, 24].

In order to deal with such restrictions, Eyre developed a semi-implicit method[19] which resolves the problems associated with both the stiffness and solvability. Furthermore Eyre proved that his algorithms are unconditionally gradient stable for the CH and also for the Allen-Cahn equation, which means that the free energy does not increase with time. Both gradient stability and the conservation of mass provide us with a simple and rational form to establish the stability criterion for the CH equation that replaced the von Neumann stability criteria. Furthermore, mostly either finite difference calculations[23, 24] or Monte Carlo simulations[25] uses periodic boundary conditions as a tentative to mimic a large system and we show here that, as concerns phase separation, that free boundary conditions are less stiff and more faster achieved.

The goal of this paper is to make a combinations of a systematic study of the CH equation in 1D, 2D and 3D using a simplification of the Eyre's method and free boundary conditions. To give a better perspective to the approach, we make also calculations with a Crank-Nicholson like (CN) implicitly scheme[26], which is unconditionally convergent in 1D and, using the concept of alternating direction interaction (ADI) method[26, 27], in 2D. These calculations demonstrate the advantage of the Eyre's method over the CN scheme. Therefore we apply Eyre's method in 3D and study the phenomenon of spinodal decomposition in three dimensions. The application to the high  $T_c$  superconductors and manganites with the study of the relevant parameters to their phase diagrams is under current investigation and will be discussed in a future work.

## II. THE PROPERTIES OF THE CAHN-HILLIARD EQUATION

In order to solve numerically Eq.(3) by means of a finite difference scheme, we need an initial condition over the entire domain,  $u(\vec{x}, 0)$ , which usually is a random function or some small fluctuations over a specific average and also some type of boundary conditions (BCs). During our simulations we have found that these initial conditions, the BCs and the size of the system greatly influence the solution  $u(\vec{x}, t)$ . The general convenient and flux-conserving boundary conditions are[20]

$$\nabla u \cdot \vec{n}|_{\vec{x} \in \partial\Omega} = (\nabla^3 u) \cdot \vec{n}|_{\vec{x} \in \partial\Omega} = 0 \quad (4)$$

where  $\vec{n}$  is the outward normal vector on the boundary of the domain  $\Omega$  which we represent by  $\partial\Omega$ . These two equations together are equivalent to

$$\nabla(\delta f / \delta u)|_{\vec{x} \in \partial\Omega} = 0. \quad (5)$$

These BCs lead to the two very important properties which will be our guide to know whether our CH numerical solutions are convergent, namely, the conservation of the total mass of the system  $M_t$ ;

$$\begin{aligned} \frac{d}{dt} M_t &= \frac{d}{dt} \int_{\Omega} u(\vec{x}, t) d\vec{x} = \int_{\Omega} \frac{\partial u(\vec{x}, t)}{\partial t} d\vec{x} \\ &= \int_{\Omega} \nabla^2 \frac{\delta f}{\delta u} d\vec{x} = \left[ \nabla \frac{\delta f}{\delta u} \right]_{\vec{x} \in \partial\Omega} = 0 \end{aligned} \quad (6)$$

and the dissipation or decrease of the total energy  $F$ ;

$$\begin{aligned} \frac{d}{dt} F(u) &= \frac{d}{dt} \int_{\Omega} f(u(\vec{x}, t)) d\vec{x} = \int_{\Omega} \frac{\delta f}{\delta u} \frac{\partial u(\vec{x}, t)}{\partial t} d\vec{x} \\ &= - \int_{\Omega} \left[ \nabla \frac{\delta f}{\delta u} \right]^2 d\vec{x} \leq 0 \end{aligned} \quad (7)$$

This last equation shows that appropriate solutions of the CH equation must dissipate energy and this is called gradient flow. Therefore a time stepping finite difference scheme is defined to be *gradient stable* only if the free energy  $F(u)$  does not increase with the time, i.e., obeys Eq.(7). Since it is not convenient to use the von Neumann stability analysis, gradient stability is regarded as the best stability criterion for finite difference numerical solutions of the CH equation [22]. Furthermore, unconditional gradient stability means that the conditions for gradient stability is satisfied for any size of time step and this will be

our guide through the simulations. This way to examine the stability of a central difference scheme by following the energy was already proposed to nonlinear problems a long time ago by Park[28]. We should mention that a similar analysis, based also on the Eyre's approach, performing numerical tests of stability and with a very complete classification scheme for the stable values of  $\Delta t$  for the CH and Allen-Cahn equation in 2D was recently developed[22].

### III. THE DISCRETIZATION METHOD

Eyre has proposed a semi-implicit method that is unconditional gradient stable if the  $V(u)$  is the usual two minima potential used in a typical GL free energy and can be divided in two parts:  $V(u) = V_c(u) + V_e(u)$  where  $V_c$  is called contractive and  $V_e$  is called expansive[19]. He showed that it is possible to achieve unconditional gradient stability if one treats the contractive part implicitly and the expansive part explicitly. In our case, since we are using  $V(u) = (u^2 - 1)^2/4$ , we have:

$$V_c(u) = \frac{u^4 + 1}{4} \quad \text{and} \quad V_e(u) = -\frac{u^2}{2}.$$

To implement Eyre's scheme we define  $U_{ijk}^n(i, j, k = 1, 2, \dots, N; n = 0, 1, 2, \dots)$  to be the approximation to  $u(\vec{x}, t)$  at location  $x = ih$ ,  $y = jh$ ,  $z = kh$  and  $t = nK$ , where  $h = \Delta x = \Delta y = \Delta z$ ,  $K = \Delta t$  and  $N = L/\Delta x$ .  $L$  is the linear size of the system, assuming to be cubic, for simplicity. With these definitions, we can write the method for the CH equation as

$$\frac{U_{ijk}^{n+1} - U_{ijk}^n}{K} = -\varepsilon^2 \nabla^4 U_{ijk}^{n+1} + \nabla^2 ((U_{ijk}^{n+1})^3 - U_{ijk}^n). \quad (8)$$

In this equation the standard centered difference approximation of the 3D Laplacian operator  $\nabla^2$  is

$$\nabla^2 U_{ijk}^n = (U_{i+1jk}^n + U_{ij+1k}^n + U_{ijk+1}^n - 6U_{ijk}^n + U_{i-1jk}^n + U_{ij-1k}^n + U_{ijk-1}^n) / h^2 \quad (9)$$

which is second order in the spatial step  $h$ . The Eq.(8) represents a large coupled set of nonlinear equations due to the cubic term. The way to go around this problem is to splitting or to linearize it at every time step. Consequently the term  $(U_{ijk}^{n+1})^3$  is transformed into  $(U_{ijk}^n)^2 U_{ijk}^{n+1}$  leading the Eq.(8) into a set of linear equations in the step of time  $n + 1$ . It has been argued that this nonlinear splitting has the smallest local truncation error[19, 22]

and therefore it will be the scheme adopted in this work. Then we finally obtain the proposed finite difference scheme for the CH equation which is linear (in the above sense), namely,

$$\frac{U_{ijk}^{n+1} - U_{ijk}^n}{K} = -\varepsilon^2 \nabla^4 U_{ijk}^{n+1} + \nabla^2 ((U_{ijk}^n)^2 U_{ijk}^{n+1} - U_{ijk}^n). \quad (10)$$

or, separating in different times to see the semi-implicit character of the approach,

$$U_{ijk}^{n+1} + K(\varepsilon^2 \nabla^4 U_{ijk}^{n+1} + \nabla^2 (U_{ijk}^n)^2 U_{ijk}^{n+1}) = U_{ijk}^n - K \nabla^2 U_{ijk}^n. \quad (11)$$

As noted by Furihata et al[20], the discrete associated boundary conditions equivalent to Eq.(4), second order in the spatial variable, become

$$U_{1jk}^n = U_{5jk}^n \quad , \quad U_{2jk}^n = U_{4jk}^n \quad (12)$$

$$U_{Njk}^n = U_{N-4jk}^n \quad , \quad U_{N-1jk}^n = U_{N-3jk}^n \quad (13)$$

and similar equations for the boundary conditions over the second and third indices representing the  $y$  and  $z$ -directions, respectively. Notice that, differently than most numerical simulations applied to physical systems[29], these boundary conditions are not periodical. Imposing periodical BCs which is common in physical applications and which is largely used to artificially simulate a larger system, would bring additional constraint to the solutions and, as we show below, the solutions will be more stiff. Therefore the above boundary conditions minimize the finite size effects and should be preferably used as shown below.

The Eq.(11) with the above boundary conditions define the finite difference scheme which we use in this present work. In the following section, we analyze the numerical results and compare with different CN semi-implicit approaches for several dimensions with the same double-well potential.

#### IV. THE RESULTS OF THE SIMULATIONS

We start with the study of the CH equation in 1D because it is faster than 2D and 3D and there are many results which can be used to compare with our simulations. The usual semi-implicit and explicit Euler's schemes for the 1D CH equation are not gradient stable and require very short time intervals  $\Delta t = K$ , while the implicit Euler's scheme is gradient stable with  $K \leq h^2/4 = 6.25 \times 10^{-6}$  [19, 21, 30]. The CN-like scheme that we will use

for comparison also suffers from this solvability restriction, and requires a minimum time interval  $K \leq h^2/9$ .

We performed calculations with linear chains of  $N = 54, 104$  and  $504$  sites and with  $\Delta x = h = 1/(N - 4)$ , and  $0 \leq x \leq 1$ . For all these cases we used  $K = h/2$  which is clearly several order of magnitude larger than typical Euler's schemes and, despite this large time step, the gradient stability is observed at all times. In Fig.1 we show the results for the total mass and the free energy  $F$  in arbitrary units as function of the running time. In fact, using shorter times as shown in Fig.1, we observe that there is an initial transient period in the time evolution before gradient stability is achieved. This can be easily seen at at most small values of  $\Delta t$  in Fig.1 for either Eyre's or CN-like methods. This transient before the stability takes place is connected to the finite size of the system, the initial conditions and the BCs.

As already mentioned, in order to compare our calculations based on Eyre's method with other schemes, we have also performed similar simulations with a widely used method[19, 21], a semi implicit CN-like scheme[26, 30]. Briefly, the CN method consists in an average of the right hand side of Eq.(3) at different times:  $1/2$  at  $n$  and  $1/2$  at  $n + 1$  what clearly results in a semi-implicit scheme in time. According to the above formula, for  $h = 1/50$ , this scheme will converge for  $K \leq 1/(2500 \times 9) \approx 1/20000$ . Indeed we can see in Fig.1 that the CN simulations agree very well with the the Eyre's results for the case with  $K = 1/50000$  and a similar transient period before the stability is achieved is observed. To compare with other studies which use the same parameters for the CH equation, we used an initial condition for the linear chain similar to one used by Furihata et al[20], namely,

$$\begin{aligned}
 U_i^0 = & 0.1\sin(2.\pi(i - 3)h) + 0.01\cos(4\pi(i - 3)h) \\
 & + 0.06\sin(4\pi(i - 3)h) + 0.02\cos(10\pi(i - 3)h)
 \end{aligned}
 \tag{14}$$

for  $3 \leq i \leq N - 2$  and  $U_i^0 = 0.03$  otherwise (at the borders). This function is shown in Fig.(2).

Now that the parameters which gradient stability is established in our system, we study the process of spinodal decomposition in 1D starting with the initial condition given by Eq.(14). Using the long time step  $\Delta t = 1/100$ , we see for the different  $U_i^n$  time profile in Fig.2, that at very few time evolution ( $n = 5$ ) the system shows a tendency to decompose in one high and other low density phases. At  $n = 10$  the difference in densities increases



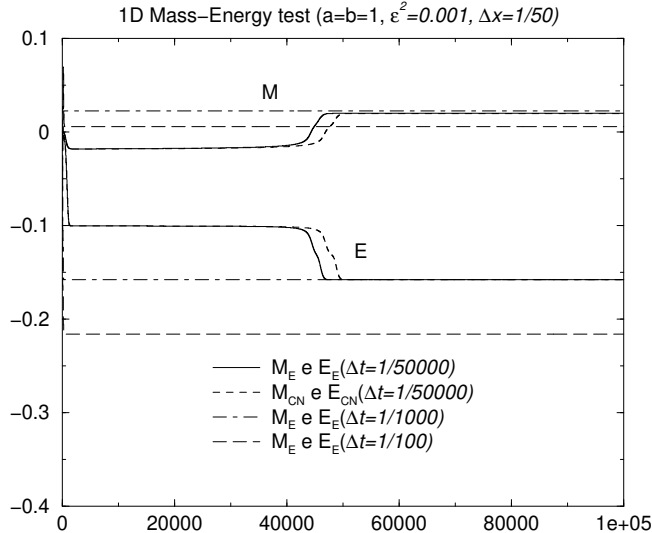


FIG. 1: Time evolution of the total mass and the total energy in arbitrary units up to  $10^5$  time steps (abscissa) by Eyre's and Crank-Nicholson's scheme at different time steps for comparison.

and the system separates in regions which almost reach the limit  $\pm 1$  values. At  $n = 50$  and  $n = 100$  the system is almost entirely separated in the two  $\pm 1$  phases. At  $n = 500$  the limit configuration is reached and the spinodal decomposition is total with the low density phase at left and the high phase at right as seen in Fig.2. Furihata et al[20] have found a similar result starting from the same initial condition using a different method. Larger systems behave in a similar fashion with the same sort of decomposition seen in Fig.(2). Notice that the system separates in two regions with different density ( $-1$  at left near  $x = 0$  and  $+1$  at the other and at  $x = 1$ ). If we had imposed periodic boundary conditions, it would impose an additional constraint and the solutions would be different than that two regions of Fig.(2), namely, three phase regions with one at the center and two of the same kind at the borders. This more complex final configuration takes more time steps to be realized as we checked, performing also calculations with periodic boundary conditions. Thus, we demonstrate that the used "free" boundary conditions are more "natural" and faster than the periodic ones and this is *an important finding which will be used in the 2D and 3D studies*.

Now, let's use what we learned above and turn our attention to the 2D problem. We worked with systems of sizes of  $104 \times 104$  and  $504 \times 504$  and again  $\Delta x = h = 1/(N - 4)$  with  $N = 104$  or  $504$ . We adopt the Eyre's scheme in the form of an alternating dimension implicit (ADI) problem[26, 27], that is, we used a half marching time step in one direction, say, in the  $x$ -direction and another half time step in the  $y$ -direction. Since most finite

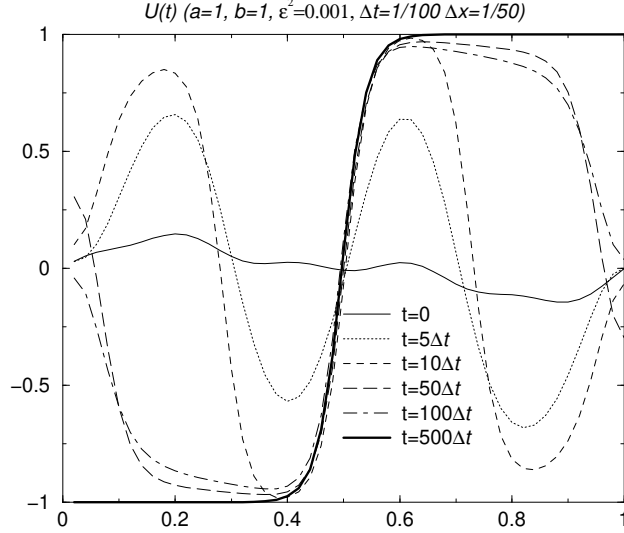


FIG. 2: The time evolution of the profile of  $U_i^n$  for different times starting at the initial condition ( $t = 0$ ) till the total spinodal decomposition is attained at  $n = 500$ . The size of the system is  $L = 1$ .

difference methods for partial differential equations like the diffusion or heat equation in 2D uses the Crank-Nicholson scheme[26, 27], we again made simulations with this scheme which is appropriate to be used in connection with the ADI[26, 27, 31].

In Fig.3 we plot the results for the 2D mass and energy in arbitrary units. We used  $\varepsilon = 0.01$  which is slightly bigger than the 1D value in order to have larger phase domains and we kept the other parameters equal. The initial conditions were chosen to be small variation around the average value  $U_{ij}^n = 0.5$  although variation around zero give the same type of result. Thus the initial condition is

$$U_{ij}^0 = 0.5 + \varepsilon \sin(\pi(i-3)20h) \sin(\pi(j-3)20h) \quad (15)$$

for  $i, j$  toward the middle and with  $U_{ij}^0 = 0.5$  toward the boundaries of our square systems. The choice of a different initial condition than  $U_{ij}^0 = 0$  is to brake the symmetry and, in this way, better identify the formation of the two  $\pm 1$  density phases (see Fig.(4) below). Studying the stability conditions, we see that the 2D system requires smaller values of  $\Delta t$  than the 1D system. This is because the boundaries are much larger in 2D and the possibility to mass and energy flow is greatly enhanced and the instability during the initial transient period is larger. For instance, the initial instabilities in the  $504 \times 504$  is even bigger than in the  $104 \times 104$  system.

The CN scheme requires at least  $\Delta t = \Delta x/1000$  which is around four times the minimum 1D value and the Eyre's requires at least  $\Delta t = \Delta x/50$ . In the simulations with the CN scheme, the mass oscillates wildly up to  $10^5$  steps and the energy has also a small increase near this number of marching time steps. The Eyre's results for  $\Delta t = \Delta x/1000$  oscillate in the beginning transient of the simulations but become gradient stable after 50000 steps when the mass and the energy stabilize. On the other hand the simulations are gradient stable and does not display any transient oscillation since the beginning for  $\Delta t = \Delta x/100$  but there is a large loss of average mass, as shown in Fig.(3).

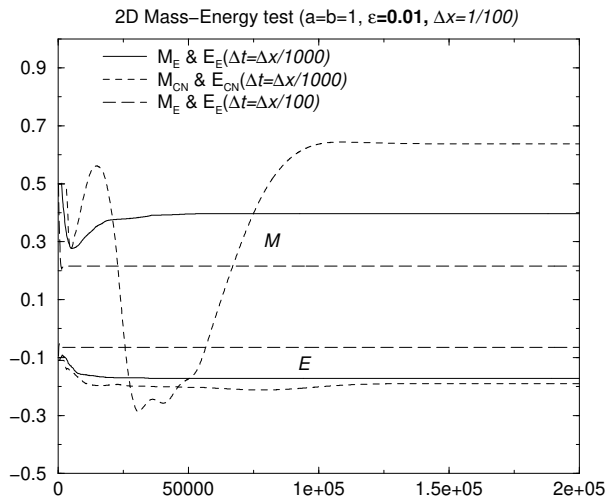


FIG. 3: The stability of the mass and the energy in 2D for the  $104 \times 104$  system by the Crank-Nicholson and Eyre's scheme for  $\Delta x = 1/100$  and different time marching steps  $\Delta t$  as specified in the legends.

As mentioned above the value of  $\varepsilon$  must be higher than that used in 1D in order to observe the phase separation phenomenon, otherwise the phase domains become very small. In order to study the phase separation through the 2D Eyre's method (with  $\Delta t = \Delta x/1000$ ), we started with the initial condition of Eq.(15). As expected from the above above analysis, around the  $1000^{th}$  time step the system start to separate into the  $\pm 1$  density phases. At the  $1000^{th}$  time step the beginning of the spinodal separation is clear as shown in Fig.(3) below.

Around the  $6000^{th}$  time step the the size of the low density islands reach an equilibrium size and the spinodal separation is complete but, the boundaries effects are large. We see a concentration of the low density phase at the borders and this effect prevents the system

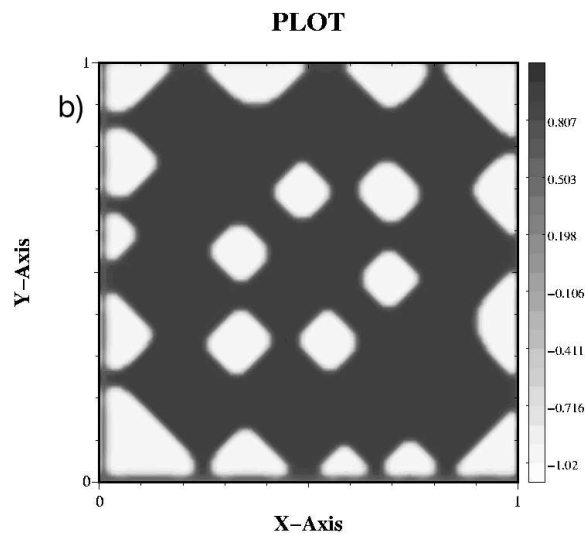
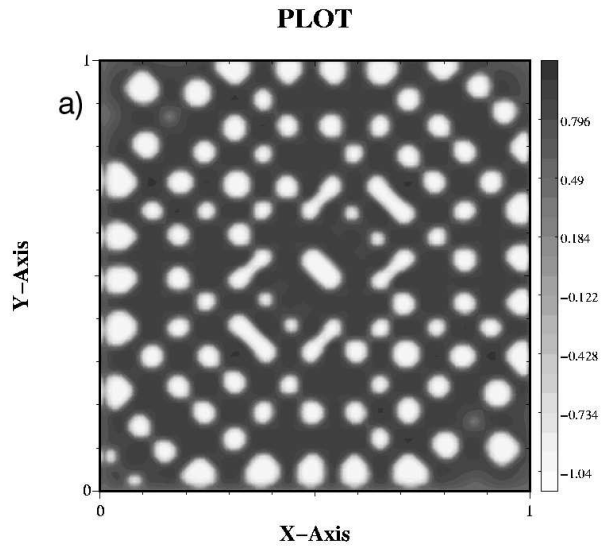


FIG. 4: At the top panel, the beginning ( $n = 2000$ ) of the spinodal decomposition with the formation of islands with the values of  $-1$  density in white in a background which tends to  $+1$  density (in black) because the initial conditions with broken symmetry. At the panel below, we see the system at a later time ( $n = 50000$ ) when it is already in equilibrium. The initial configuration is that given by Eq.(15).

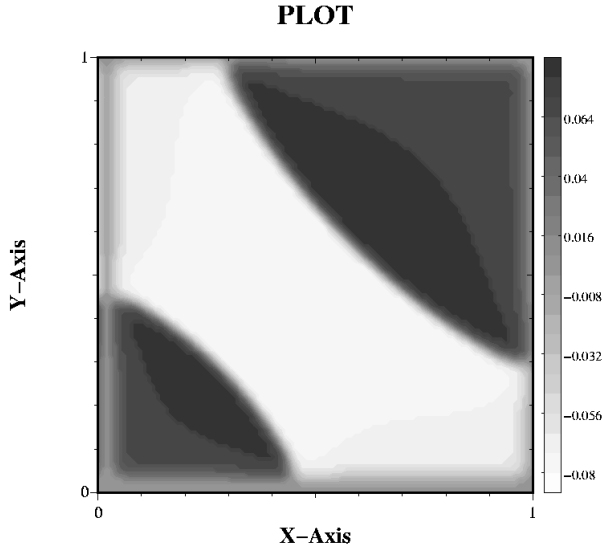


FIG. 5: The same type of figure of Fig.(4) but for  $V(u)$  coefficients  $a = 0.6^2$  and  $b = 4.0^2$  (instead of  $a = 1$  and  $b = 1$ , which produces two easily separated phases with  $u = \pm 0.15$ ) after the equilibrium is achieved ( $n = 40000$ ).

to reach a total phase separation as we have seen in 1D (see Fig.(2)). This shows how the boundary effects are very strong and more significant in 2D. After this time step the system achieves a stable configuration without appreciable changes up to  $10^6$  time steps. Below we show a snap shot of this equilibrium configuration at  $n = 50000$ . Similar results were obtained with the  $504 \times 504$  system but in this case there is a proportional increase of the islands size and the equilibrium situation is similar to five times blow up of Fig.(4). Simulations with a larger value of the non-linear coefficient  $b$  (see discussion after Eq.(2)) enhances the mass flow inside the system and it is possible to achieve complete phase separation at an earlier time, exactly as seen in 1D, but with two phases with smaller values than  $\pm 1$ . In Fig.(5) we plot a situation with  $a = 0.6$  and  $b = 4.0$ . In this case there is an easy mass flow through the system and an state of complete phase separation is reached around  $n = 40000$ . Notice that the system reaches the equilibrium with nonperiodical BCs.

We turn now to analyze the 3D system. As we have already found in the 2D case, the problem of mass/energy flow is largely enhanced through the boundaries. To deal with such effects, we have to use a small (compared with those used in the 2D case) marching time

step of  $\Delta t = \Delta x/10000$  with  $\Delta x = 1/100$  for the  $(104)^3$  system to minimize errors in the derivatives near the boundaries. Notice that this time step is much smaller than the one in 1D and one-two orders of magnitude smaller than in 2D. This is small but still feasible to reach the interesting dynamics even in a typical PC of 1GHz. Since Eyre’s method is very efficient and faster than the majority of other methods used in 3D, this is the only approach that we used in 3D. The generalization of basic Euler or Runge-Kutta methods to the CH equation in 3D are much more slower, and we can see why there are very few studies of the CH equation in 3D. Indeed the values of  $\Delta t \approx 10^{-6}$  used in our 3D simulations are of the same order of magnitude of typical Euler’s method[19, 21, 30] used in 1D simulation as we discussed in the beginning of this section. The adopted initial condition for the 3D system is:

$$U_{ijk}^0 = 0.01 + \varepsilon \sin(\pi(i - 3)20h) \sin(\pi(j - 3)20h) \sin(\pi(k - 3)20h). \quad (16)$$

We used an average small initial mass of 0.01 just to minimize the mass flow through the boundaries and indeed the mass remains very stable for up to  $4 \times 10^4$  time steps, when it starts a slightly increase.

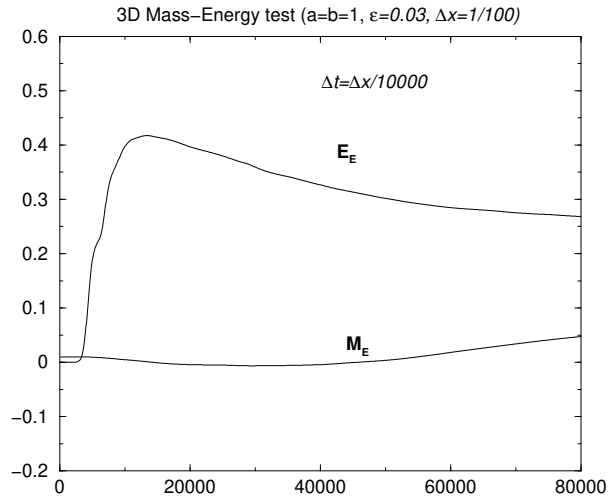


FIG. 6: The stability of the mass and the energy in 3D for the  $104^3$  system by the Eyre’s scheme for  $\Delta x, y, z = 1/100$ .

As concerns the energy, it remains stable for the first step of the simulations but the boundaries effects are manifested near the time step 4000 and increases up to step 13000. During this transient period of time, although the mass is stable, the simulations are not,

as one can conclude by the energy increase in this interval as shown in Fig.(6). After this time interval ( $n \approx 13000$ ) the system stabilizes itself and remains gradient stable up to the rest of the calculations (up to  $n = 80000$ ) as can be seen by the decrease of the energy in Fig.(6). Comparison with the 1D and 2D systems reveals clearly that the stability is more difficult to be established as the dimensionality increases, as it is natural when one uses any finite difference scheme. As Fig.(6) shows, the system relax from the initial conditions and becomes uniform around  $n = 3000$ . Around  $n = 6000$  a spinodal decomposition is happening and the oscillation in the densities forms an almost uniform pattern as shown in the top panel of Fig.(7). This figure shows the configuration of the middle plane in the z-direction ( $k = 52$ ) of the  $104 \times 104 \times 104$ . At the down panel of Fig.(7) we show a snap-shot of  $n = 8000$  which shows the beginning of of the phase separation process as the time flows. Above  $n = 20000$  the two phases start to segregate and this segregation process is smooth and unconditionally gradient stable as seen in Fig.(8).

At much later time like  $n = 40000$  the phase separation phenomenon is on the way. At  $n = 80000$  the phase separation is almost total in the plane passing by the middle of the system, as it is shown in the down panel of Fig.(8).

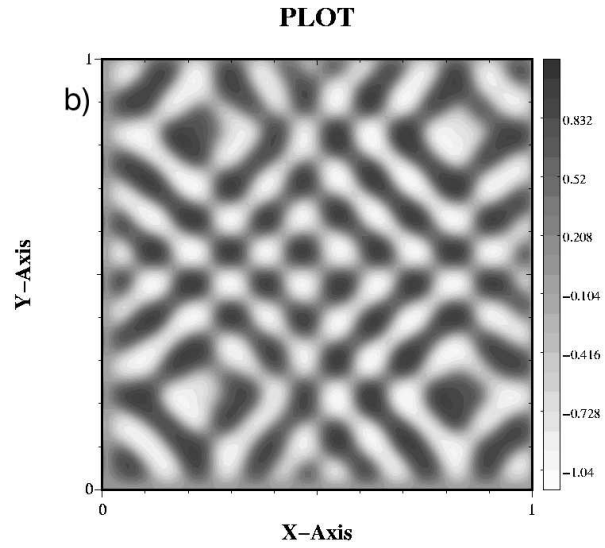
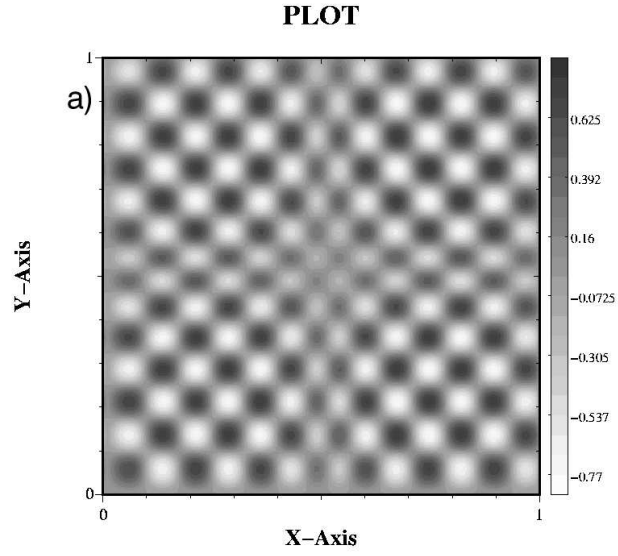


FIG. 7: After relaxing from the initial condition (Eq.(16)), we show at the top panel the beginning ( $n = 6000$ ) of the spinodal decomposition with the formation of small islands with the  $\pm 1$  values because the initial condition with broken symmetry. At the down panel, the system at a later time ( $n = 8000$ ) during the process of phase separation.



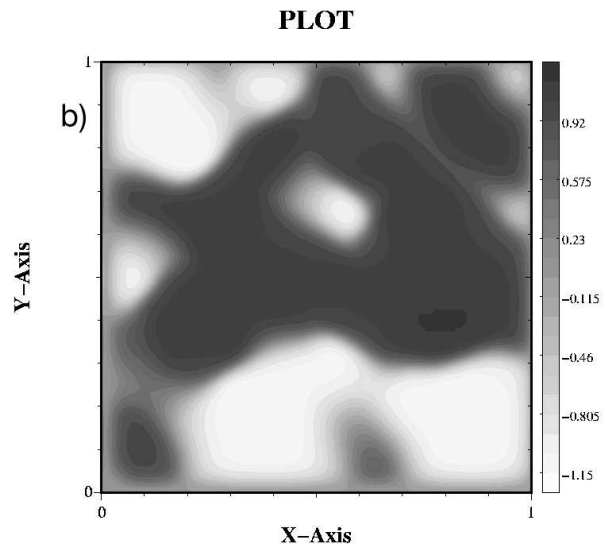
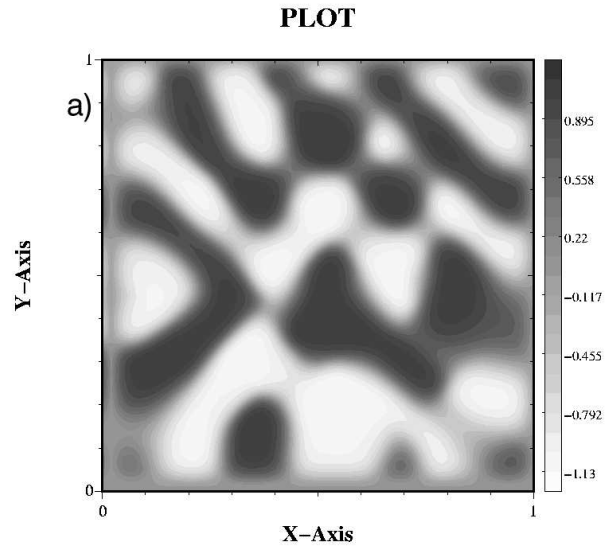


FIG. 8: The continuation of Fig.(7) for many time steps later. On the top panel we plot the case for  $n = 40000$  and on the down panel the  $n = 80000$ .

## V. CONCLUSION

We have shown in this work that the semi-implicit method due to Eyre, which divides the potential  $V(u)$  in two parts and treats the contractive part implicitly and the expansive ex-

PLICITLY combined with free boundary conditions achieves unconditional gradient stability in 1D, 2D and 3D. The method also allows the use of very long marching time steps, compared with usual explicit or implicit Euler's schemes, what is convenient because it captures very easily the short and long dynamics, characteristic of the Cahn-Hilliard equation. Our simulations have demonstrated that gradient stability and spinodal decomposition is achieved faster than the normal Euler and Crank-Nicholson methods what is highly desirable specially in 3D where normal methods fail to capture the long dynamics due to the required very short time steps. The use of "nonflow" free BCs are more appropriated and also converges faster to a final equilibrium configuration than the widely used periodic BCs.

We believe that the present systematic study may be pertinent to the several branches of physics. The fast scheme developed here are suitable to the study of the spinodal dynamics and also to high correlated electron systems with phase separation. We expect therefore, to perform these works in the near future.

## VI. ACKNOWLEDGMENT

We gratefully acknowledge partial financial aid from Brazilian agencies CNPq and FAPERJ.

- 
- [1] I.M. Lifshitz and V.V.Slyozov, *J. Phys. Chem. Solids* **19**, 35 (1961).
  - [2] P.C. Hohenberg and B.I Halperin, *Rev. Mod. Phys.* **49**, 435 (1977).
  - [3] J.D. Gunton, M. San Miguel, and P.S. Sahni, in "Phase Transitions and Critical Phenomena" Vol. 8, edited by C. Domb and J.L. Lebowitz (New York, Academic Press, 1983).
  - [4] A.J. Bray, *Adv. Phys.* **43**, 347 (1994).
  - [5] J.W. Cahn and J.E. Hilliard, *J. Chem. Phys.* **28**, 258 (1958).
  - [6] J.M.Traquada, B.J. Sternlieb, J.D, Axe, Y. Nakamura, and S. Uchida, *Nature (London)*,**375**, 561 (1995).
  - [7] A. Bianconi N. L Saini, A. Lanzara, M. Missori, T. Rossetti, H. Oyanagi, H. Yamaguchi, K. Oka, T.Ito, *Phys. Rev. Lett.* **76**, 3412 (1996).
  - [8] C. Howald, P. Fournier, and A. Kapitulnik, *Phys. Rev.* **B64**, 100504 (2001).

- [9] S. H. Pan, J. P. O'Neal, R. L. Badzey, C. Chamon, H. Ding, J. R. Engelbrecht, Z. Wang, H. Eisaki, S. Uchida, A.K. Gupta, K. W. Ng, E. W. Hudson, K. M. Lang, J. C. Davis *Nature*, 413, 282-285 (2001) and cond-mat/0107347.
- [10] Yu.N. Ovchinnikov, S.A. Wolf, V.Z. Kresin, *Phys. Rev.* **B63**, 064524, (2001), and *Physica* **C341-348**, 103, (2000).
- [11] E.V.L. de Mello, M.T.D. Orlando, E.S. Caixeiro, J.L. González, and E. Baggio-Saitovich, *Phys. Rev.* **B66**, 092505 (2002).
- [12] D. Mihailovic, V.V. Kabanov, K.A. Müller, *Europhys. Lett.* **57**, 254 (2002).
- [13] E.V.L. de Mello, E.S. Caixeiro, and J.L. González, *Phys. Rev.* **B67**, 024502 (2003).
- [14] See several articles in "Proceedings of the Workshop on Intrinsic Multiscale Structure and Dynamics of Complex Electronic Oxides", I.C.T.P., A.R. Bishop, S.R. Shenoy, and S. Sridhar, Eds., World Scientific, New Jersey (2002).
- [15] E.S. Caixeiro, J.L. González, and E.V.L. de Mello. *Phys. Rev.* **B69**, 024521 (2004).
- [16] E. Dagotto, T. Hotta and, A. Moreo, *Phys. Rep.* **344**, 1 (2001).
- [17] E. Dagotto, J. Burgy, A. Moreo, *Sol. St. Comm.* **126**, 9, (2003).
- [18] J.S Kim, K. Kang and J.S. Lowengrub, "Conservative multigrid methods for Cahn-Hilliard fluids", *J. Comput. Phys.* In press
- [19] D.J. Eyre, "Unconditionally gradient stable time marching the Cahn-Hilliard equation" preprint, (1998), and "An Unconditional stable one-step scheme for gradient systems" (<http://www.math.utah.edu/~eyre/research/methods/stable.ps>) (1998).
- [20] D. Furihata and T. Matuso, RIMS Preprint no.1271, Kyoto University, (2000).
- [21] C.M. Elliot and D.A. French, *IMA J. Appl. Math*, **38**, 97 (1987)
- [22] B.P. Vollmayr-Lee and A.D. Rutenberg, cond-mat/0308174, (2003).
- [23] A. Chakrabarti, R. Toral, J.D. Gunton, and M. Muthukumar, *Phys. Rev. Lett.* **63**, 2072 (2001).
- [24] R. Toral, A. Chakrabarti and J.D. Gunton, *Phys. Rev.* **A45**, R2147 (1992).
- [25] A. Milchev, D.W. Heermann, and K. Binder, *Acta Metal* 36, 377 (1988).
- [26] W.F. Ames, "Numerical Methods for Partial Differential Equations", Academic Press, New York (1977).
- [27] J. Douglas Jr., R. Duran and P. Pietra, in "Numerical Approximation of Partial Differential Equations", E. Ortiz, ed., North-Holland, Amsterdam (1987).

- [28] K.C. Park in "Computer and Structure", Vol.7, pp 343-353, Pergamon Press, London (1977).
- [29] J. Wang, D.Y. Xing, J. Dong and P.H. Hor, Phys. Rev. **B62**, 9827 (2000).
- [30] J.H. Mathews, "Numerical Methods for Mathematics, Science, and Engineering", Prentice Hall, Englewood Cliffs, N.J. (1992).
- [31] C.E. Elliot in "Mathematical Models for Phase Change Problems", J.F. Rodriguez Ed., Birkhäuser Verlag, Basel (1989).